First Measurement of the Angular Coefficients of Drell-Yan e+e- Pairs in the Z Mass Region from pp Collisions at s=1.96TeV

First Measurement of the Angular Coefficients of Drell-Yan e^+e^- Pairs in the Z Mass Region from $p\bar{p}$ Collisions at $\sqrt{s} = 1.96$ TeV

T. Aaltonen,[21] B. Álvarez González,[9,x] S. Amerio,[41a] D. Amidei,[32] A. Anastassov,[36] A. Annovi,[17] J. Antos,[12] G. Apollinari,[15] J. A. Appel,[15] A. Apresyan,[46] T. Arisawa,[56] A. Artikov,[13] J. Asaadi,[51] W. Ashmanskas,[15] B. Auerbach,[59] A. Aurisano,[51] F. Azfar,[40] W. Badgett,[15] A. Barbaro-Galtieri,[26] V. E. Barnes,[46] B. A. Barnett,[23] P. Barria,[44b,44a] P. Bartos,[12] M. Bauce,[41b,41a] G. Bauer,[30] F. Bedeschi,[44a] D. Beecher,[28] S. Behari,[23] G. Bellettini,[44b,44a] J. Bellinger,[58] D. Benjamin,[14] A. Beretvas,[15] A. Bhatti,[48] M. Binkley,[15,a] D. Bisello,[41b,41a] I. Bizjak,[28,bb] K. R. Bland,[5] B. Blumenfeld,[23] A. Bocci,[14] A. Bodek,[47] D. Bortoletto,[46] J. Boudreau,[45] A. Boveia,[11] B. Brau,[15,b] L. Brigliadori,[6b,6a] A. Brisuda,[12] C. Bromberg,[33] E. Brucken,[21] M. Bucciantonio,[44b,44a] J. Budagov,[13] H. S. Budd,[47] S. Budd,[22] K. Burkett,[15] G. Busetto,[41b,41a] P. Bussey,[19] A. Buzatu,[31] C. Calancha,[29] S. Camarda,[4] M. Campanelli,[33] M. Campbell,[32] F. Canelli,[11,15] A. Canepa,[43] B. Carls,[22] D. Carlsmith,[58] R. Carosi,[44a] S. Carrillo,[16,l] S. Carron,[15] B. Casal,[9] M. Casarsa,[15] A. Castro,[6b,6a] P. Catastini,[15] D. Cauz,[52a] V. Cavaliere,[44b,44a] M. Cavalli-Sforza,[4] A. Cerri,[26,g] L. Cerrito,[28,r] Y. C. Chen,[1] M. Chertok,[7] G. Chiarelli,[44a] G. Chlachidze,[15] F. Chlebana,[15] K. Cho,[25] D. Chokheli,[13] J. P. Chou,[20] W. H. Chung,[58] Y. S. Chung,[47] C. I. Ciobanu,[42] M. A. Ciocci,[44b,44a] A. Clark,[18] G. Compostella,[41b,41a] M. E. Convery,[15] J. Conway,[7] M. Corbo,[42] M. Cordelli,[17] C. A. Cox,[7] D. J. Cox,[7] F. Crescioli,[44b,44a] C. Cuenca Almenar,[59] J. Cuevas,[9,x] R. Culbertson,[15] D. Dagenhart,[15] N. d'Ascenzo,[42,v] M. Datta,[15] P. de Barbaro,[47] S. De Cecco,[49a] G. De Lorenzo,[4] M. Dell'Orso,[44b,44a] C. Deluca,[4] L. Demortier,[48] J. Deng,[14,d] M. Deninno,[6a] F. Devoto,[21] M. d'Errico,[41b,41a] A. Di Canto,[44b,44a] B. Di Ruzza,[44a] J. R. Dittmann,[5] M. D'Onofrio,[27] S. Donati,[44b,44a] P. Dong,[15] M. Dorigo,[52a] T. Dorigo,[41a] K. Ebina,[56] A. Elagin,[51] A. Eppig,[32] R. Erbacher,[7] D. Errede,[22] S. Errede,[22] N. Ershaidat,[42,aa] R. Eusebi,[51] H. C. Fang,[26] S. Farrington,[40] M. Feindt,[24] J. P. Fernandez,[29] C. Ferrazza,[44b,44c,44d] R. Field,[16] G. Flanagan,[46,t] R. Forrest,[7] M. J. Frank,[5] M. Franklin,[20] J. C. Freeman,[15] Y. Funakoshi,[56] I. Furic,[16] M. Gallinaro,[48] J. Galyardt,[10] J. E. Garcia,[18] A. F. Garfinkel,[46] P. Garosi,[44b,44c] H. Gerberich,[22] E. Gerchtein,[15] S. Giagu,[49b,49a] V. Giakoumopoulou,[3] P. Giannetti,[44a] K. Gibson,[45] C. M. Ginsburg,[15] N. Giokaris,[3] P. Giromini,[17] M. Giunta,[44a] G. Giurgiu,[23] V. Glagolev,[13] D. Glenzinski,[15] M. Gold,[35] D. Goldin,[51] N. Goldschmidt,[16] A. Golossanov,[15] G. Gomez,[9] G. Gomez-Ceballos,[30] M. Goncharov,[30] O. González,[29] I. Gorelov,[35] A. T. Goshaw,[14] K. Goulianos,[48] S. Grinstein,[4] C. Grosso-Pilcher,[11] R. C. Group,[55,15] J. Guimaraes da Costa,[20] Z. Gunay-Unalan,[33] C. Haber,[26] S. R. Hahn,[15] E. Halkiadakis,[50] A. Hamaguchi,[39] J. Y. Han,[47] F. Happacher,[17] K. Hara,[53] D. Hare,[50] M. Hare,[54] R. F. Harr,[57] K. Hatakeyama,[5] C. Hays,[40] M. Heck,[24] J. Heinrich,[43] M. Herndon,[58] S. Hewamanage,[5] D. Hidas,[50] A. Hocker,[15] W. Hopkins,[15,h] D. Horn,[24] S. Hou,[1] R. E. Hughes,[37] M. Hurwitz,[11] U. Husemann,[59] N. Hussain,[31] M. Hussein,[33] J. Huston,[33] G. Introzzi,[44a] M. Iori,[49b,49a] A. Ivanov,[7,p] E. James,[15] D. Jang,[10] B. Jayatilaka,[14] E. J. Jeon,[25] M. K. Jha,[6a] S. Jindariani,[15] W. Johnson,[7] M. Jones,[46] K. K. Joo,[25] S. Y. Jun,[10] T. R. Junk,[15] T. Kamon,[51] P. E. Karchin,[57] A. Kasmi,[5] Y. Kato,[39,o] W. Ketchum,[11] J. Keung,[43] V. Khotilovich,[51] B. Kilminster,[15] D. H. Kim,[25] H. S. Kim,[25] H. W. Kim,[25] J. E. Kim,[25] M. J. Kim,[17] S. B. Kim,[25] S. H. Kim,[53] Y. K. Kim,[11] N. Kimura,[56] M. Kirby,[15] S. Klimenko,[16] K. Kondo,[56] D. J. Kong,[25] J. Konigsberg,[16] A. V. Kotwal,[14] M. Kreps,[24] J. Kroll,[43] D. Krop,[11] N. Krumnack,[5,m] M. Kruse,[14] V. Krutelyov,[51,e] T. Kuhr,[24] M. Kurata,[53] S. Kwang,[11] A. T. Laasanen,[46] S. Lami,[44a] S. Lammel,[15] M. Lancaster,[28] R. L. Lander,[7] K. Lannon,[37,w] A. Lath,[50] G. Latino,[44b,44a] T. LeCompte,[2] E. Lee,[51] H. S. Lee,[11] J. S. Lee,[25] S. W. Lee,[51,y] S. Leo,[44b,44a] S. Leone,[44a] J. D. Lewis,[15] A. Limosani,[14,s] C.-J. Lin,[26] J. Linacre,[40] M. Lindgren,[15] E. Lipeles,[43] A. Lister,[18] D. O. Litvintsev,[15] C. Liu,[45] Q. Liu,[46] T. Liu,[15] S. Lockwitz,[59] N. S. Lockyer,[43] A. Loginov,[59] D. Lucchesi,[41b,41a] J. Lueck,[24] P. Lujan,[26] P. Lukens,[15] G. Lungu,[48] J. Lys,[26] R. Lysak,[12] R. Madrak,[15] K. Maeshima,[15] K. Makhoul,[30] P. Maksimovic,[23] S. Malik,[48] G. Manca,[27,c] A. Manousakis-Katsikakis,[3] F. Margaroli,[46] C. Marino,[24] M. Martínez,[4] R. Martínez-Ballarín,[29] P. Mastrandrea,[49a] M. Mathis,[23] M. E. Mattson,[57] P. Mazzanti,[6a] K. S. McFarland,[47] P. McIntyre,[51] R. McNulty,[27,j] A. Mehta,[27] P. Mehtala,[21] A. Menzione,[44a] C. Mesropian,[48] T. Miao,[15] D. Mietlicki,[32] A. Mitra,[1] H. Miyake,[53] S. Moed,[20] N. Moggi,[6a] M. N. Mondragon,[15,l] C. S. Moon,[25] R. Moore,[15] M. J. Morello,[15] J. Morlock,[24] P. Movilla Fernandez,[15] A. Mukherjee,[15] Th. Muller,[24] P. Murat,[15] M. Mussini,[6b,6a] J. Nachtman,[15,n] Y. Nagai,[53] J. Naganoma,[56] I. Nakano,[1] A. Napier,[54] J. Nett,[51] C. Neu,[55] M. S. Neubauer,[22] J. Nielsen,[26,f] L. Nodulman,[2] O. Norniella,[22] E. Nurse,[28] L. Oakes,[40] S. H. Oh,[14] Y. D. Oh,[25] I. Oksuzian,[55] T. Okusawa,[39] R. Orava,[21] L. Ortolan,[4] S. Pagan Griso,[41b,41a] C. Pagliarone,[52a] E. Palencia,[9,g] V. Papadimitriou,[15] A. A. Paramonov,[2] J. Patrick,[15] G. Pauletta,[52b,52a] M. Paulini,[10] C. Paus,[30] D. E. Pellett,[7] A. Penzo,[52a] T. J. Phillips,[14] G. Piacentino,[44a] E. Pianori,[43] J. Pilot,[37] K. Pitts,[22] C. Plager,[8] L. Pondrom,[58] K. Potamianos,[46] O. Poukhov,[13,a] F. Prokoshin,[13,z] A. Pronko,[15] F. Ptohos,[17,i] E. Pueschel,[10] G. Punzi,[44b,44a] J. Pursley,[58] A. Rahaman,[45] V. Ramakrishnan,[58] N. Ranjan,[46] I. Redondo,[29]

P. Renton,[40] M. Rescigno,[49a] F. Rimondi,[6b,6a] L. Ristori,[45,15] A. Robson,[19] T. Rodrigo,[9] T. Rodriguez,[43] E. Rogers,[22] S. Rolli,[54] R. Roser,[15] M. Rossi,[52a] F. Rubbo,[15] F. Ruffini,[44b,44a] A. Ruiz,[9] J. Russ,[10] V. Rusu,[15] A. Safonov,[51] W. K. Sakumoto,[47] Y. Sakurai,[56] L. Santi,[52b,52a] L. Sartori,[44a] K. Sato,[53] V. Saveliev,[42,v] A. Savoy-Navarro,[42] P. Schlabach,[15] A. Schmidt,[24] E. E. Schmidt,[15] M. P. Schmidt,[59,a] M. Schmitt,[36] T. Schwarz,[7] L. Scodellaro,[9] A. Scribano,[44b,44a] F. Scuri,[44a] A. Sedov,[46] S. Seidel,[35] Y. Seiya,[39] A. Semenov,[13] F. Sforza,[44b,44a] A. Sfyrla,[22] S. Z. Shalhout,[7] T. Shears,[27] P. F. Shepard,[45] M. Shimojima,[53,u] S. Shiraishi,[11] M. Shochet,[11] I. Shreyber,[34] A. Simonenko,[13] P. Sinervo,[31] A. Sissakian,[13,a] K. Sliwa,[54] J. R. Smith,[7] F. D. Snider,[15] A. Soha,[15] S. Somalwar,[50] V. Sorin,[4] P. Squillacioti,[15] M. Stancari,[15] M. Stanitzki,[59] R. St. Denis,[19] B. Stelzer,[31] O. Stelzer-Chilton,[31] D. Stentz,[36] J. Strologas,[35] G. L. Strycker,[32] Y. Sudo,[53] A. Sukhanov,[16] I. Suslov,[13] K. Takemasa,[53] Y. Takeuchi,[53] J. Tang,[11] M. Tecchio,[32] P. K. Teng,[1] J. Thom,[15,h] J. Thome,[10] G. A. Thompson,[22] E. Thomson,[43] P. Ttito-Guzmán,[29] S. Tkaczyk,[15] D. Toback,[51] S. Tokar,[12] K. Tollefson,[33] T. Tomura,[53] D. Tonelli,[15] S. Torre,[17] D. Torretta,[15] P. Totaro,[41a] M. Trovato,[44b,44a,44d] Y. Tu,[43] F. Ukegawa,[53] S. Uozumi,[25] A. Varganov,[32] F. Vázquez,[16,l] G. Velev,[15] C. Vellidis,[3] M. Vidal,[29] I. Vila,[9] R. Vilar,[9] J. Vizán,[9] M. Vogel,[35] G. Volpi,[44b,44a] P. Wagner,[43] R. L. Wagner,[15] T. Wakisaka,[39] R. Wallny,[8] S. M. Wang,[1] A. Warburton,[31] D. Waters,[28] M. Weinberger,[51] W. C. Wester III,[15] B. Whitehouse,[54] D. Whiteson,[43,d] A. B. Wicklund,[2] E. Wicklund,[15] S. Wilbur,[11] F. Wick,[24] H. H. Williams,[43] J. S. Wilson,[37] P. Wilson,[15] B. L. Winer,[37] P. Wittich,[15,h] S. Wolbers,[15] H. Wolfe,[37] T. Wright,[32] X. Wu,[18] Z. Wu,[5] K. Yamamoto,[39] J. Yamaoka,[14] T. Yang,[15] U. K. Yang,[11,q] Y. C. Yang,[25] W.-M. Yao,[26] G. P. Yeh,[15] K. Yi,[15,n] J. Yoh,[15] K. Yorita,[56] T. Yoshida,[39,k] G. B. Yu,[14] I. Yu,[25] S. S. Yu,[15] J. C. Yun,[52a] A. Zanetti,[52a] Y. Zeng,[14] and S. Zucchelli[6b,6a]

(CDF Collaboration)

[1]*Institute of Physics, Academia Sinica, Taipei, Taiwan 11529, Republic of China*
[2]*Argonne National Laboratory, Argonne, Illinois 60439, USA*
[3]*University of Athens, 157 71 Athens, Greece*
[4]*Institut de Fisica d'Altes Energies, ICREA, Universitat Autonoma de Barcelona, E-08193, Bellaterra (Barcelona), Spain*
[5]*Baylor University, Waco, Texas 76798, USA*
[6a]*Istituto Nazionale di Fisica Nucleare Bologna, I-40127 Bologna, Italy*
[6b]*University of Bologna, I-40127 Bologna, Italy*
[7]*University of California, Davis, Davis, California 95616, USA*
[8]*University of California, Los Angeles, Los Angeles, California 90024, USA*
[9]*Instituto de Fisica de Cantabria, CSIC-University of Cantabria, 39005 Santander, Spain*
[10]*Carnegie Mellon University, Pittsburgh, Pennsylvania 15213, USA*
[11]*Enrico Fermi Institute, University of Chicago, Chicago, Illinois 60637, USA*
[12]*Comenius University, 842 48 Bratislava, Slovakia; Institute of Experimental Physics, 040 01 Kosice, Slovakia*
[13]*Joint Institute for Nuclear Research, RU-141980 Dubna, Russia*
[14]*Duke University, Durham, North Carolina 27708, USA*
[15]*Fermi National Accelerator Laboratory, Batavia, Illinois 60510, USA*
[16]*University of Florida, Gainesville, Florida 32611, USA*
[17]*Laboratori Nazionali di Frascati, Istituto Nazionale di Fisica Nucleare, I-00044 Frascati, Italy*
[18]*University of Geneva, CH-1211 Geneva 4, Switzerland*
[19]*Glasgow University, Glasgow G12 8QQ, United Kingdom*
[20]*Harvard University, Cambridge, Massachusetts 02138, USA*
[21]*Division of High Energy Physics, Department of Physics, University of Helsinki and Helsinki Institute of Physics, FIN-00014, Helsinki, Finland*
[22]*University of Illinois, Urbana, Illinois 61801, USA*
[23]*The Johns Hopkins University, Baltimore, Maryland 21218, USA*
[24]*Institut für Experimentelle Kernphysik, Karlsruhe Institute of Technology, D-76131 Karlsruhe, Germany*
[25]*Center for High Energy Physics: Kyungpook National University, Daegu 702-701, Korea; Seoul National University, Seoul 151-742, Korea; Sungkyunkwan University, Suwon 440-746, Korea; Korea Institute of Science and Technology Information, Daejeon 305-806, Korea; Chonnam National University, Gwangju 500-757, Korea; Chonbuk National University, Jeonju 561-756, Korea*
[26]*Ernest Orlando Lawrence Berkeley National Laboratory, Berkeley, California 94720, USA*
[27]*University of Liverpool, Liverpool L69 7ZE, United Kingdom*
[28]*University College London, London WC1E 6BT, United Kingdom*
[29]*Centro de Investigaciones Energeticas Medioambientales y Tecnologicas, E-28040 Madrid, Spain*
[30]*Massachusetts Institute of Technology, Cambridge, Massachusetts 02139, USA*

[31]Institute of Particle Physics: McGill University, Montréal, Québec, Canada H3A 2T8;
Simon Fraser University, Burnaby, British Columbia, Canada V5A 1S6;
University of Toronto, Toronto, Ontario, Canada M5S 1A7;
and TRIUMF, Vancouver, British Columbia, Canada V6T 2A3
[32]University of Michigan, Ann Arbor, Michigan 48109, USA
[33]Michigan State University, East Lansing, Michigan 48824, USA
[34]Institution for Theoretical and Experimental Physics, ITEP, Moscow 117259, Russia
[35]University of New Mexico, Albuquerque, New Mexico 87131, USA
[36]Northwestern University, Evanston, Illinois 60208, USA
[37]The Ohio State University, Columbus, Ohio 43210, USA
[1]Okayama University, Okayama 700-8530, Japan
[39]Osaka City University, Osaka 588, Japan
[40]University of Oxford, Oxford OX1 3RH, United Kingdom
[41a]Istituto Nazionale di Fisica Nucleare, Sezione di Padova-Trento, I-35131 Padova, Italy
[41b]University of Padova, I-35131 Padova, Italy
[42]LPNHE, Universite Pierre et Marie Curie/IN2P3-CNRS, UMR7585, Paris, F-75252 France
[43]University of Pennsylvania, Philadelphia, Pennsylvania 19104, USA
[44a]Istituto Nazionale di Fisica Nucleare Pisa, I-56127 Pisa, Italy
[44b]University of Pisa, I-56127 Pisa, Italy
[44c]University of Siena, I-56127 Pisa, Italy
[44d]Scuola Normale Superiore, I-56127 Pisa, Italy
[45]University of Pittsburgh, Pittsburgh, Pennsylvania 15260, USA
[46]Purdue University, West Lafayette, Indiana 47907, USA
[47]University of Rochester, Rochester, New York 14627, USA
[48]The Rockefeller University, New York, New York 10065, USA
[49a]Istituto Nazionale di Fisica Nucleare, Sezione di Roma 1, I-00185 Roma, Italy
[49b]Sapienza Università di Roma, I-00185 Roma, Italy
[50]Rutgers University, Piscataway, New Jersey 08855, USA
[51]Texas A&M University, College Station, Texas 77843, USA
[52a]Istituto Nazionale di Fisica Nucleare Trieste/Udine, I-34100 Trieste, I-33100 Udine, Italy
[52b]University of Trieste/Udine, I-33100 Udine, Italy
[53]University of Tsukuba, Tsukuba, Ibaraki 305, Japan
[54]Tufts University, Medford, Massachusetts 02155, USA
[55]University of Virginia, Charlottesville, Virginia 22906, USA
[56]Waseda University, Tokyo 169, Japan
[57]Wayne State University, Detroit, Michigan 48201, USA
[58]University of Wisconsin, Madison, Wisconsin 53706, USA
[59]Yale University, New Haven, Connecticut 06520, USA
(Received 30 March 2011; published 15 June 2011)

We report on the first measurement of the angular distributions of final state electrons in $p\bar{p} \to \gamma^*/Z \to e^+e^- + X$ events produced in the Z boson mass region at $\sqrt{s} = 1.96$ TeV. The data sample collected by the CDF II detector for this result corresponds to 2.1 fb^{-1} of integrated luminosity. The angular distributions are studied as a function of the transverse momentum of the electron-positron pair and show good agreement with the Lam-Tung relation, consistent with a spin-1 description of the gluon, and demonstrate that, at high values of the transverse momentum, Z bosons are produced via quark-antiquark annihilation and quark-gluon Compton processes.

DOI: 10.1103/PhysRevLett.106.241801 PACS numbers: 13.38.Dg, 12.38.Bx, 13.85.Qk, 14.70.Hp

We report on a study of the angular distributions of final state electrons in $p\bar{p} \to \gamma^*/Z \to e^+e^- + X$ Drell-Yan events to probe Z boson production mechanisms. In quantum chromodynamics (QCD) at the order of α_s, this occurs either through the annihilation process with a gluon (G) in the final state ($q\bar{q} \to \gamma^*/ZG$) or via the Compton process with a quark in the final state ($qG \to \gamma^*/Zq$). The emission of final state q/G gives γ^*/Z transverse momentum [1] [we define the production $P_T = P_T(\gamma^*/Z) = P_T(e^+e^-)$ before final state radiation].

The general expression for the angular distribution [2] is described by the polar (θ) and azimuthal (ϕ) angles of the decay electron in the Collins-Soper (CS) frame [3]. When integrated over $\cos\theta$ or ϕ, respectively, the decay-electron angular distribution is described by

$$\frac{d\sigma}{d\cos\theta} \propto (1 + \cos^2\theta) + \frac{1}{2}A_0(1–3\cos^2\theta) + A_4\cos\theta, \quad (1)$$

$$\frac{d\sigma}{d\phi} \propto 1 + \beta_3 \cos\phi + \beta_2 \cos 2\phi + \beta_7 \sin\phi + \beta_5 \sin 2\phi, \quad (2)$$

where $\beta_3 = 3\pi A_3/16$, $\beta_2 = A_2/4$, $\beta_7 = 3\pi A_7/16$, and $\beta_5 = A_5/4$. The A_0 and A_4 are extracted from Eq. (1), and A_2 and A_3 are extracted from Eq. (2), while A_5 and A_7 are expected to be zero [2].

Perturbative QCD (pQCD) makes definite predictions for the angular coefficients $A_{0,2,3,4}$ (A_0 and A_2 are the same for γ^* or Z exchange, and A_3 and A_4 originate from the γ^*/Z interference). For the $q\bar{q} \to \gamma^*/ZG$ annihilation process, pQCD at the order of α_s predicts that the angular coefficients A_0 and A_2 are equal [4–7] and can be analytically described by

$$A_0^{q\bar{q}} = A_2^{q\bar{q}} = P_T^2/(M_{e^+e^-}^2 + P_T^2). \quad (3)$$

At higher order, there are small deviations from the above expression [Eq. (3)] which depend on parton distribution functions (PDFs) and dilepton rapidity (y) [1].

For the $qG \to \gamma^*/Zq$ Compton process, A_0 and A_2 depend on PDFs and y. However, in pQCD at the order of α_s, when averaged over y, A_0 and A_2 are approximately described [8,9] by

$$A_0^{qG} = A_2^{qG} \approx 5P_T^2/(M_{e^+e^-}^2 + 5P_T^2). \quad (4)$$

At the order of α_s, the Lam-Tung relation ($A_0 = A_2$) [10] is valid for both $q\bar{q}$ and qG processes [5]. Fixed-order pQCD calculations at the order of α_s^2 [2], as well as QCD resummation calculations to all orders [6], indicate that violations of the Lam-Tung relation are small. The Lam-Tung relation is valid only for vector (spin-1) gluons. It is badly broken for scalar (spin-0) gluons [11]. Therefore, confirmation of the Lam-Tung relation is a fundamental test of the vector gluon nature of QCD and is equivalent to a measurement of the spin of the gluon. A previous determination of the gluon spin was made from a study of 3-jet events ($e^+e^- \to q\bar{q}G$) in e^+e^- annihilation [12].

To date, the Lam-Tung relation has been tested only at fixed-target experiments using samples of low mass Drell-Yan dilepton pairs at relatively low transverse momentum. In this region, nonperturbative higher-twist effects can be significant [13,14]. Some experiments report large violations [8,14–16], and one experiment [17] is consistent with the Lam-Tung relation. Here we report on the first test of the Lam-Tung relation at a large dilepton mass and high transverse momentum, where nonperturbative higher-twist effects are expected to be negligible.

Fixed-order pQCD calculations [2] and Monte Carlo (MC) simulations at next-to-leading order [e.g., DYRAD [18] and MADGRAPH [19], and PYTHIA in $(Z+1)$-jet mode [20]] indicate that there is a significant ($\approx 30\%$) contribution of the Compton process to the production of γ^*/Z bosons at the Tevatron. Therefore, as shown in Fig. 3, these calculations yield values of A_0 and A_2 which are larger than the pure annihilation process prediction [Eq. (3)]. Similar results are predicted by POWHEG [21], a next-to-leading order MC simulation with additional parton showering, and FEWZ [22] which is a next-to-next-to-leading order QCD calculation.

In contrast, the default, LO version of PYTHIA [23] and VBP [24] (an MC generator based on QCD resummation) predict values of A_0 and A_2 which are close to Eq. (3) (which is correct only if the $q\bar{q}$ process is dominant). The RESBOS [25] MC generator, which is also based on QCD resummation, predicts values of A_0 and A_2 close to Eq. (3) at low P_T and larger values (close to the predictions of fixed-order pQCD) at high P_T, as shown in Fig. 3. Therefore, measurements of A_0 and A_2 as a function of P_T elucidate the relative contributions between the annihilation and Compton processes.

In this Letter, we report on the first measurement of the angular coefficients A_0, A_2, A_3, and A_4, for $p\bar{p} \to \gamma^*/Z \to e^+e^- + X$ events in the Z boson mass region ($66 < M_{ee} < 116$ GeV/c^2) produced at $\sqrt{s} = 1.96$ TeV. We also report on the first test of the Lam-Tung relation at high transverse momentum.

The sample used corresponds to an integrated luminosity of 2.1 fb^{-1} collected by the CDF II detector at Fermilab [26] during 2004–2007. Charged particle directions and momenta are measured by an open-cell drift chamber, a silicon vertex detector, and an intermediate silicon layer in a 1.4 T magnetic field. Projective-tower-geometry calorimeters and outer muon detectors enclose the magnetic tracking volume. The coverage of open-cell drift chamber tracking in pseudorapidity is $|\eta| < 1.2$ [1]. Reconstructed tracks are used to determine the $p\bar{p}$ collision point along the beam line, which is required to be within $z = \pm 60$ cm of the center of the detector. The energies and directions [1] of electrons, photons, and jets are measured by two separate calorimeters: central ($|\eta| < 1.1$) and plug ($1.1 < |\eta| < 3.6$). Each calorimeter has an electromagnetic compartment with a shower maximum detector followed by a hadronic compartment. Three topologies of e^+e^- pairs are considered: two central electrons (CC), one central and one plug electron (CP), and two plug electrons (PP). Events with at least one electron with high E_T are selected on-line. Off-line refined selection requires the electron to have $E_T > 25$ GeV for CC and PP events, and $E_T > 20$ GeV for CP events in the fiducial regions of the calorimeters, the central ($|\eta_e| < 1.1$) and plug ($1.2 < |\eta_e| < 2.8$). To minimize background, the second electron candidate is required to have $E_T > 15$ GeV for CC, $E_T > 25$ GeV for PP, and $E_T > 20$ GeV for CP events. The selection criteria listed above are the same as in the related previous publication [27] of the Z rapidity distribution but are augmented in this analysis with the additional requirement that both electrons have an associated track in the silicon vertex detector. The data sample consists of about 140 000 events. The fractional contribution of the total QCD background (2-jet events misidentified as Drell-Yan pairs) to the number of

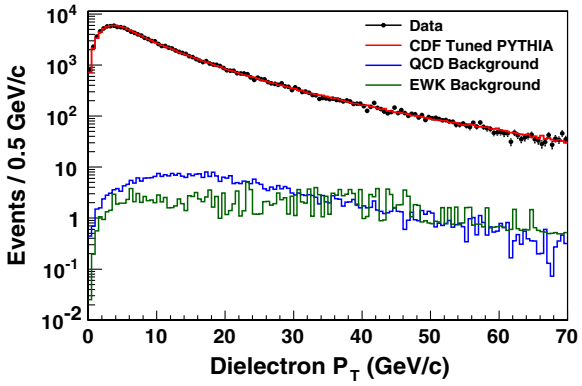

FIG. 1 (color online). Dielectron P_T spectrum of data, default (CDF tuned) PYTHIA prediction, and backgrounds (QCD and electroweak processes). The mass range corresponds to $66 < M_{ee} < 116$ GeV$/c^2$.

selected events is 0.3%. This is determined by studying the distribution of transverse energy in a cone surrounding the center of the electromagnetic cluster in the calorimeter. The total background from electroweak (WW, WZ, W + jets, and $Z \to \tau^+\tau^-$) and $t\bar{t}$ processes is estimated from simulation to be 0.2%.

The effect of the acceptance on the angular distributions is modeled by using the PYTHIA MC generator [23] combined with a GEANT [28] simulation of the CDF detector. The PYTHIA generator includes a LO QCD interaction ($q\bar{q} \to \gamma^*/Z$), initial state QCD radiation, parton shower fragmentation, the $\gamma^*/Z \to e^+e^-$ decay, and photon radiation from the final state. The version of PYTHIA used at CDF has additional *ad hoc* tuning [23] (referred to as default PYTHIA) in order to accurately represent the γ^*/Z boson transverse momentum distribution measured in the data. Further tuning was introduced in order to ensure that the MC simulation correctly described the rapidity, as well as the correlations between rapidity and transverse momentum that are observed in the data. To reconstruct the simulated events in the same way as the data, the calorimeter energy scale, resolutions, and selection efficiencies used in the detector simulation are tuned [27] by using data. Figure 1 shows the dielectron P_T spectrum for data, the default PYTHIA prediction, and the backgrounds. There is good agreement between the data and PYTHIA prediction. Figure 2 shows the cosθ distribution for the data and the default PYTHIA prediction and its ratio.

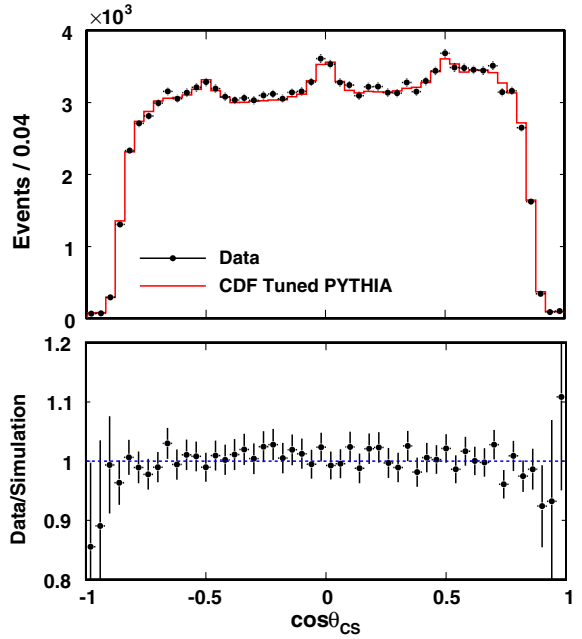

FIG. 2 (color online). The cosθ distribution of data and default (CDF tuned) PYTHIA prediction.

The analysis is performed in five bins of transverse momentum as shown in Table I. For each transverse momentum range, data and MC simulated events are binned in cosθ and ϕ. The MC events are reweighted to generate the expected angular distributions (cosθ and ϕ) for a range of values of A_0 and A_4, and A_2 and A_3, respectively. The angular distributions from the reweighted MC events are compared to the data in the reconstructed level, and the angular coefficients which give a maximum log-likelihood value are determined as the best coefficients to describe the data. The A_0 and A_4 are determined by the comparison of the data to MC distributions in cosθ, and the A_2 and A_3 are determined in ϕ. The normalization factor of the data to MC events is also included as one of fit parameters. The results are shown in Fig. 3 and in Table I with statistical and systematic uncertainties. The correlation between extracted values of A_0 and A_2, and A_3 and A_4, is negligible. The systematic uncertainties originating from backgrounds, electron identification efficiency, silicon vertex detector tracking efficiency, boson P_T and rapidity modeling, and modeling of detector material are considered. The dominant source is the background estimation. Most of the systematic uncertainties are discussed in Ref. [27], and the effect of these uncertainties on the shape of the angular distribution is small.

TABLE I. The measured angular coefficients (measured value $\pm$stat error $\pm$ syst error). The mean P_T of the events in the five bins is 4.8, 14.1, 26.0, 42.9, and 73.7 GeV$/c$, respectively.

P_T bin	A_0 ($\times 10^{-1}$)	A_2 ($\times 10^{-1}$)
0–10	$0.17 \pm 0.14 \pm 0.07$	$0.16 \pm 0.26 \pm 0.06$
10–20	$0.42 \pm 0.25 \pm 0.07$	$-0.01 \pm 0.35 \pm 0.16$
20–35	$0.86 \pm 0.39 \pm 0.08$	$0.52 \pm 0.51 \pm 0.29$
35–55	$3.11 \pm 0.59 \pm 0.10$	$2.88 \pm 0.84 \pm 0.19$
>55	$4.97 \pm 0.61 \pm 0.10$	$4.83 \pm 1.24 \pm 0.02$
P_T bin	A_3 ($\times 10^{-1}$)	A_4 ($\times 10^{-1}$)
0–10	$-0.04 \pm 0.12 \pm 0.01$	$1.10 \pm 0.10 \pm 0.01$
10–20	$0.18 \pm 0.16 \pm 0.01$	$1.01 \pm 0.17 \pm 0.01$
20–35	$0.14 \pm 0.24 \pm 0.01$	$1.56 \pm 0.26 \pm 0.01$
35–55	$-0.19 \pm 0.41 \pm 0.04$	$0.52 \pm 0.42 \pm 0.03$
>55	$-0.47 \pm 0.56 \pm 0.02$	$0.85 \pm 0.50 \pm 0.05$

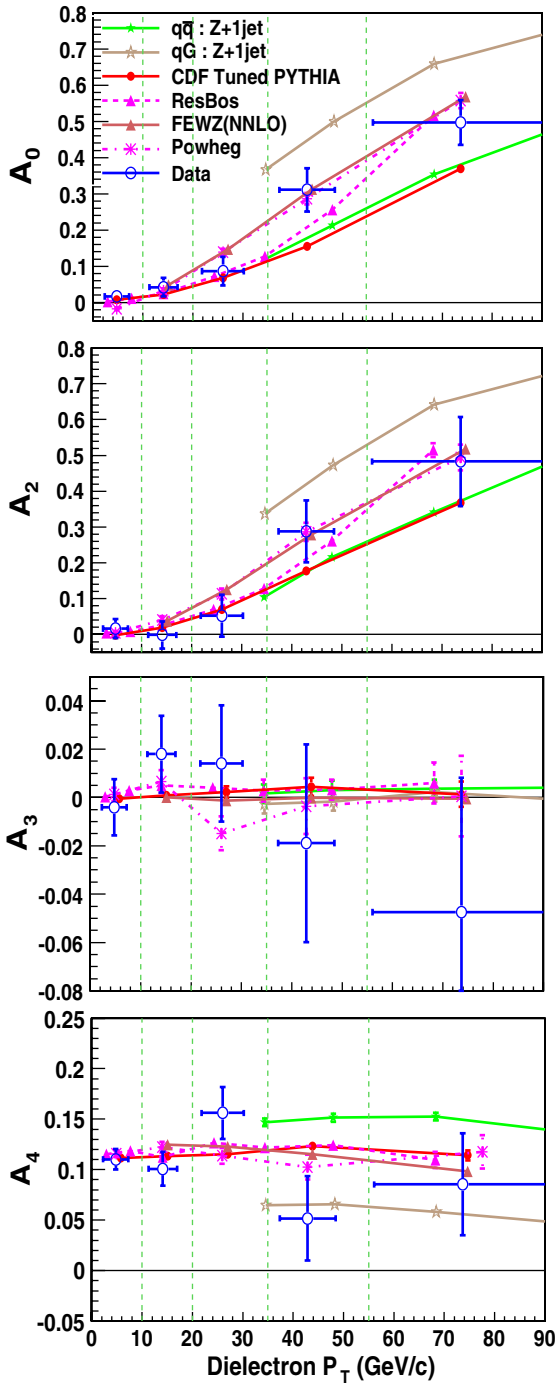

FIG. 3 (color online). Comparison of the measured values of A_0, A_2, A_3, and A_4 (for $66 < M_{ee} < 116$ GeV/c^2), shown with statistical and systematic uncertainties combined in quadrature, to theory predictions. The data are plotted at the mean P_T of the events for each bin. The last bin corresponds to $P_T > 55$ GeV/c with no upper limit. The horizontal uncertainty is the rms of the transverse momenta in each bin. Agreement [29] is found with the predictions of FEWZ and POWHEG (shown) and also with DYRAD, MADGRAPH, and PYTHIA $(Z + 1)$-jet MC simulations (not shown). The data do not favor [29] the predictions of default PYTHIA and VBP. Also shown are the pure $q\bar{q} \to \gamma^*/ZG$ annihilation diagram prediction and the $qG \to \gamma^*/Zq$ Compton process prediction from the PYTHIA $(Z + 1)$-jet MC simulation.

The data are in good agreement with the Lam-Tung relation $A_0 - A_2 = 0$, which is expected in QCD with vector gluons. The values of $A_0 - A_2$ for the five P_T bins are 0.00 ± 0.03, 0.04 ± 0.05, 0.03 ± 0.07, 0.02 ± 0.11, and 0.01 ± 0.14 (statistical and systematic uncertainties combined), which average to $\langle A_0 - A_2 \rangle = 0.02 \pm 0.02$. At low P_T the measured values of A_0 and A_2 are well described by the $q\bar{q} \to \gamma^*/ZG$ annihilation function [Eq. (3)]. At high P_T the larger values show that both the annihilation and Compton processes contribute to the cross section [29]. Our results are in agreement [29] with fixed-order perturbation theory calculations including DYRAD [18], MADGRAPH [19], PYTHIA $Z + 1$ jet [20], POWHEG [21], and FEWZ [22] (all of these give similar predictions). We find that the values of A_3 and A_4 are in agreement with the predictions of all models (A_4 is calculated with $\sin^2\theta_W = 0.232$).

In summary, we present the first measurement of the angular coefficients in the production of γ^*/Z bosons at large transverse momenta and the first test of the Lam-Tung relation at high transverse momentum. We find good agreement with the predictions of the QCD fixed-order perturbation theory and with the Lam-Tung relation $A_0 = A_2$. The measurements presented here are statistically limited. An analysis with larger samples in both muon and electron channels is currently under way. A comparison of these results with future measurements at the LHC would provide additional tests of production mechanisms since the contribution of the Compton process $(qG \to \gamma^*/Zq)$ at the LHC is expected to be larger.

We thank the Fermilab staff and the technical staffs of the participating institutions for their vital contributions. This work was supported by the U.S. Department of Energy and National Science Foundation; the Italian Istituto Nazionale di Fisica Nucleare; the Ministry of Education, Culture, Sports, Science and Technology of Japan; the Natural Sciences and Engineering Research Council of Canada; the National Science Council of the Republic of China; the Swiss National Science Foundation; the A. P. Sloan Foundation; the Bundesministerium für Bildung und Forschung, Germany; the Korean World Class University Program, the National Research Foundation of Korea; the Science and Technology Facilities Council and the Royal Society, United Kingdom; the Institut National de Physique Nucleaire et Physique des Particules/CNRS; the Russian Foundation for Basic Research; the Ministerio de Ciencia e Innovación, and Programa Consolider-Ingenio 2010, Spain; the Slovak R&D Agency; and the Academy of Finland.

[a]Deceased.
[b]Visitor from University of Massachusetts Amherst, Amherst, MA 01003, USA.

[c]Visitor from Istituto Nazionale di Fisica Nucleare, Sezione di Cagliari, 09042 Monserrato (Cagliari), Italy.
[d]Visitor from University of California Irvine, Irvine, CA 92697, USA.
[e]Visitor from University of California Santa Barbara, Santa Barbara, CA 93106, USA.
[f]Visitor from University of California Santa Cruz, Santa Cruz, CA 95064, USA.
[g]Visitor from CERN, CH-1211 Geneva, Switzerland.
[h]Visitor from Cornell University, Ithaca, NY 14853, USA.
[i]Visitor from University of Cyprus, Nicosia CY-1678, Cyprus.
[j]Visitor from University College Dublin, Dublin 4, Ireland.
[k]Visitor from University of Fukui, Fukui City, Fukui Prefecture, Japan 910-0017.
[l]Visitor from Universidad Iberoamericana, Mexico D.F., Mexico.
[m]Visitor from Iowa State University, Ames, IA 50011, USA.
[n]Visitor from University of Iowa, Iowa City, IA 52242, USA.
[o]Visitor from Kinki University, Higashi-Osaka City, Japan 577-8502.
[p]Visitor from Kansas State University, Manhattan, KS 66506, USA.
[q]Visitor from University of Manchester, Manchester M13 9PL, United Kingdom.
[r]Visitor from Queen Mary, University of London, London, E1 4NS, United Kingdom.
[s]Visitor from University of Melbourne, Victoria 3010, Australia.
[t]Visitor from Muons, Inc., Batavia, IL 60510, USA.
[u]Visitor from Nagasaki Institute of Applied Science, Nagasaki, Japan.
[v]Visitor from National Research Nuclear University, Moscow, Russia.
[w]Visitor from University of Notre Dame, Notre Dame, IN 46556, USA.
[x]Visitor from Universidad de Oviedo, E-33007 Oviedo, Spain.
[y]Visitor from Texas Tech University, Lubbock, TX 79609, USA.
[z]Visitor from Universidad Tecnica Federico Santa Maria, 110v Valparaiso, Chile.
[aa]Visitor from Yarmouk University, Irbid 211-63, Jordan.
[bb]On leave from J. Stefan Institute, Ljubljana, Slovenia.

[1] In the CDF detector frame, the positive z axis is define by the proton beam direction. The pseudorapidity is $\eta = -\ln\tan(\theta/2)$. For an e^+e^- pair, $P_T = P\sin\theta$ and $E_T = E\sin\theta$, where θ is the polar angle between the particle direction and the z axis. For an e^+e^- pair, $y = \frac{1}{2}\ln\frac{E+P_z}{E-P_z}$, where P and P_z are the magnitude and z component of the momentum, respectively, and E and $M_{e^+e^-}$ are the energy and mass, respectively.
[2] E. Mirkes and J. Ohnemus, Phys. Rev. D **50**, 5692 (1994); **51**, 4891 (1995).
[3] J. C. Collins and D. E. Soper, Phys. Rev. D **16**, 2219 (1977). The CS frame is the center of mass of the γ^*/Z, where the z axis is defined as the bisector of the p and $\bar{p}$ beams. The polar angle is defined as the angle of the positive lepton with respect to the proton direction.
[4] J. C. Collins, Phys. Rev. Lett. **42**, 291 (1979).
[5] D. Boer and W. Vogelsang, Phys. Rev. D **74**, 014004 (2006).
[6] E. L. Berger, J. Qiu, and R. A. Rodriguez-Pedraza, Phys. Lett. B **656**, 74 (2007).
[7] A. Bodek, Eur. Phys. J. C **67**, 321 (2010).
[8] S. Falciano *et al.* (NA10 Collaboration), Z. Phys. C **31**, 513 (1986).
[9] J. Lindfors, Phys. Scr. **20**, 19 (1979).
[10] C. S. Lam and W. K. Tung, Phys. Lett. **80B**, 228 (1979).
[11] $A_0 - A_2 \approx -2$ in the Gottfried-Jackson frame; see N. Arteaga-Romero, A. Nicolaidis, and J. Silva, Phys. Rev. Lett. **52**, 172 (1984).
[12] R. Brandelik *et al.* (TASSO Collaboration), Phys. Lett. **97B**, 453 (1980) (their data were consistent with spin-1 gluons but 3.8 standard deviations from the prediction for spin-0 gluons).
[13] D. Boer, Phys. Rev. D **60**, 014012 (1999).
[14] J. S. Conway *et al.* (E615 Collaboration), Phys. Rev. D **39**, 92 (1989).
[15] M. Guanziroli *et al.* (NA10 Collaboration), Z. Phys. C **37**, 545 (1988).
[16] J. G. Heinrich *et al.* (E615 Collaboration), Phys. Rev. D **44**, 1909 (1991).
[17] L. Y. Zhu *et al.* (FNAL-E866/NuSea Collaboration), Phys. Rev. Lett. **99**, 082301 (2007).
[18] W. T. Giele, E. W. N. Glover, and D. A. Kosower, Nucl. Phys. **B403**, 633 (1993).
[19] F. Maltoni and T. Stelzer, J. High Energy Phys. 02 (2003) 027. We use CTEQ6.6 PDFs for MADGRAPH.
[20] T. Sjöstrand *et al.*, J. High Energy Phys. 05 (2006) 026. We use the PYTHIA 6.4 $(Z+1)$-jet matrix element event generator (MSEL = 13) with parton showering [MSTP(61) = 2 and MSTJ(41) = 1] and CTEQ5L PDFs. We also generate the PYTHIA 6.4 $Z+1$ jet without any parton showering [MSTP(61) = 0 and MSTJ(41) = 0]. The PYTHIA $Z+1$ jet without parton showering gives the same angular coefficients as the PYTHIA $Z+1$ jet with parton showering.
[21] We have used the most recent version of POWHEG. See S. Alioli, P. Nason, C. Oleari, and E. Re, J. High Energy Phys. 01 (2011) 095, with CTEQ6.6 PDFs.
[22] K. Melnikov and F. Petriello, Phys. Rev. Lett. **96**, 231803 (2006); Phys. Rev. D **74**, 114017 (2006), with MSTW2008 next-to-next-to-leading order PDFs.
[23] Default (CDF tuned) PYTHIA (6.216) includes the $q\bar{q}$ and part of the qG (t-channel only) processes. T. Sjøstrand *et al.*, J. High Energy Phys. 05 (2006) 026. We use the default (MSEL = 11) LO matrix element $(Z+0$ jet) with CTEQ5L PDFs. The parton showering produces the boson P_T. The CDF standard W/Z P_T tuning parameters are MSTP(91) = 1, PARP(91) = 2.10, and PARP(93) = 15 for the low P_T Gaussian smearing, with PART(62) = 1.25 and PARP(62) = 0.2 for the P_T evolution in the 7–25 GeV region. The underlying event is included as Tune A. The QED parton showering uses the same machinery as QCD parton showering aside from coupling differences.

[24] R. K. Ellis and S. Veseli, Nucl. Phys. **B511**, 649 (1998). We use CTEQ6.6 PDFs with VBP.
[25] F. Landry, R. Brock, P. M. Nadolsky, and C.-P. Yuan, Phys. Rev. D **67**, 073016 (2003). We use CTEQ6.6 PDFs with RESBOS.
[26] D. Acosta *et al.* (CDF Collaboration), Phys. Rev. D **71**, 032001 (2005).
[27] T. Aaltonen *et al.* (CDF Collaboration) Phys. Lett. B **692**, 232 (2010); Jiyeon Han, Ph.D. thesis, University of Rochester [Report No. FERMILAB-THESIS-2008-65].
[28] GEANT: CERN Program Library Long Writeup W5013.
[29] For the four highest P_T bins, the χ^2 values for A_0 are 11.7, 9.4, 5.6, and 3.7 for default PYTHIA ($q\bar{q}$ and t channel qG), VBP, RESBOS, and FEWZ ($q\bar{q} + qG$), respectively.